IFS #185

ALFVÉN CONTINUUM WITH TOROIDICITY

S. Riyopoulos and *S. Mahajan*

Institute for Fusion Studies

The University of Texas at Austin

Austin, Texas 78712

Abstract

The symmetry property of the magnetohydrodynamic wave propagation operator is utilized to express the toroidal eigenmodes as a superposition of the mutually orthogonal cylindrical modes. Because of the degeneracy among cylindrical modes with the same frequency but resonant surfaces of different helicity the toroidal perturbation produces a zeroth order mixing of the above modes. The toroidal eigenmodes of frequency ω_o^2 have multiple resonant surfaces, with each surface shifted relative to its cylindrical position and carrying a multispectral content. Thus a single helicity toroidal antenna of frequency ω_o couples strongly to all different helicity resonant surfaces with matching local Alfvén frequency. Zeroth order coupling between modes in the continuum and global Alfvén modes also results from toroidicity and degeneracy. The perturbation technique used in this study is the MHD counterpart of the quantum mechanical methods and is applicable through the entire range of the MHD spectrum.

I. Introduction

The magnetohydrodynamic activity in magnetically confined inhomogeneous current-carrying plasmas has been the subject of extensive studies. The entire spectrum of solutions of the second order differential equation governing the wave propagation is well understood in cylindrical geometry. The unstable subclass of Alfvén modes $\omega^2 \lesssim 0$ and especially these with $k_{\|} \sim 0$ (nothing but a manifestation of the unstable "kink" modes) was originally studied[1-4] due to its profound importance in determining the gross MHD stability. It was only lately that the class of the stable modes $\omega^2 > 0$ came under the scope of extensive research in association with plasma heating via Alfvén waves.[5-20] The singularity of the differential equation at the resonant layer $r = r_0$ defined by $\omega^2 = \omega_A^2(r_0) \equiv k_{\|}^2 v_A^2(r_0)$ gives rise to a continuum part in the spectrum[5-8] lying between $(k_{\|}^2 v_A^2)_{\min} < \omega^2 < (k_{\|}^2 v_A^2)_{\max}$. The wave excitation and heating in this regime, involving rather complicated mathematics due to the singularity, has been studied and demonstrated both analytically[7,10,11] numerically[12,13,21,22] and experimentally.[23,24] An important aspect of the more recent theoretical work is the appreciation that the discrete stable part of the spectrum existing below the continuum frequencies $\omega^2 < (k_{\|}^2 v_A^2)_{\min}$ and representing the non-singular global Alfvén modes offers a more promising method of plasma heating.[13,14]

The inclusion of toroidicity effects is necessary for a more realistic picture of heating schemes in many fusion devices but nevertheless not trivial. Direct solutions of the differential equation by expansions in powers of the inverse aspect ration ϵ around the cylindrical configurations become complicated by the dependence of the toroidal metric on the poloidal single θ. Solving the equations in generalized flux coordinates, a method used in proving the *existence of* resonant surfaces and continuum in systems with only one degree of symmetry[9] (i.e. toroidal) is not an easy task either.

In this paper we develop a perturbation theory that circumvents direct integration by utilizing the orthogonality and completeness property of the cylindrical set of solutions.

The toroidal modes are expanded in a series of cylindrical eigenmodes with the expansion coefficients defined through the proper integral definition of the inner product, following a procedure analogous to the quantum-mechanical perturbation techniques.

The method can be used to find the asymptotic form of the toroidal eigenmodes everywhere in the frequency spectrum. The results however are more dramatic when applied in the continuum part of the spectrum due to the inherent degeneracy among modes corresponding to distinct resonant layers of different helicity but the same local Alfvén frequency. The frequency correction in the resulting toroidal continuum is small of order ϵ, but the radial profile of the toroidal modes involves a zeroth order mixing among degenerate cylindrical modes in the continuum plus possible degenerate global Alfvén modes. Thus the new toroidal eigenmodes exhibit multihelicity multiresonant surfaces which from the practical point of view has the following implication: a single helicity, monochromatic antenna that, in cylindrical geometry, would excite the resonant surface of the same frequency and helicity, in toroidal geometry excites to about the same order all the different helicity surfaces with local Alfvén frequency matching that of the antenna. Thus energy may be severely absorbed in layers outside than the intended resonant layer (i.e., the one with the helicity of the antenna) as it has already been verified numerically.[21,22]

Inclusion of parallel electron dynamics leads to a fourth order differential equation resolving the singularity and discretizing the continuum[10,11,14] (with or without electron Landau damping). The new solutions however preserve the qualitative properties of the ideal MHD solutions in that the modes corresponding to the old continuum are severely localized around the associated resonant layers in contrast to the "spread out" global modes, and that the distance between two successive frequencies in the old continuum regime remains small. It has also been shown[10,11] that the resulting mode conversion into a kinetic Alfvén wave near the resonant layer and the electron Landau damping leads to the same energy absorption as in the ideal MHD treatment, thus the conclusions derived from our MHD treatment have a general validity.

The accidental degeneracy between the global Alfvén modes and the continuum part of the spectrum is of practical importance in the presence of dissipation caused either by finite electron mass effects[14] or resistivity.[15] The excitation of higher helicity global modes from a lower helicity antenna will greatly improve energy deposition as the continuum part of the spectrum is suppressed by dissipation while global modes are only slightly affected excited to large amplitude cavity modes that appear as poles in the antenna impedance.[12,23] The inclusion of resistivity in particular, that leads to a departure from the self-adjoint MHD formalism utilized in our perturbation techniques, should be addressed separately and is beyond the scope of this work.

We diverge here to note that the class of the marginally stable $\omega^2 \simeq 0$ kink modes also constitutes a set of accidentally degenerate modes subject to destabilization by toroidal effects. The methods that will be developed in the next sections can also be used to provide an estimate for the modification in the growth rate due to the toroidicity.

The remaining of this paper is organized as follows: In Sec. II the equations of the wave propagation in toroidal geometry are derived. In Sec. III we prove the symmetry and orthogonality conditions that are necessary to carry out the perturbation theory. In Sec. IV the toroidal modes are expanded to first order in ϵ in cylindrical modes. In Sec. V we carry the perturbation theory to higher order by including the toroidicity effects in the differential operator. We conclude and summarize in Sec. VI.

II. Wave Propagation Equation with Toroidicity

It is convenient to introduce a field aligned set of basis vectors $(\hat{e}_r, \hat{e}_\perp, \hat{e}_{||})$ related to the cylindrical (or pseudotoroidal) basis by

$$\begin{pmatrix} \hat{e}_r \\ \hat{e}_\perp \\ \hat{e}_{||} \end{pmatrix} = T \begin{pmatrix} \hat{e}_r \\ \hat{e}_\theta \\ \hat{e}_z \end{pmatrix} , \quad T = \begin{pmatrix} 1 & 0 & 0 \\ 0 & \cos a & \sin a \\ 0 & \sin a & \cos a \end{pmatrix} ,$$

where a is the angle between the field lines and the toroidal direction (Fig. 1). The wave

propagation equation takes the form

$$\mathcal{L}\ \mathcal{E} - \frac{\omega^2}{c^2} K\ \mathcal{E} = 0 \tag{1}$$

with $\mathcal{E} = (E_r, E_\perp, E_\parallel)$; K the cold plasma dielectric tensor and $\mathcal{L}$ is the field aligned representation of the cylindrical $\nabla \times \nabla \times$ operator

$$\mathcal{L} = T\left[\nabla \times \nabla \times\right] T^{-1}.$$

In the Alfvén frequency regime $\omega \lesssim \Omega_i$, where Ω_i is the ion cylcotron frequency, $E_\parallel$ is shorted out by the large parallel conductivity and can be neglected compared to E_r, $E_\perp$ thus Eq. (1) is reduced to

$$\left(L - \frac{\omega^2}{c^2} K\right)\chi = 0 \tag{2a}$$

with

$$\chi = \begin{pmatrix} E_r(r,\theta) \\ E_\perp(r,\theta) \end{pmatrix} e^{ikz}, \quad K = \begin{pmatrix} c^2/v_A^2 & i\ (\omega/\Omega_i) \quad c^2/v_A^2 \\ -i\ (\omega/\Omega_i)\ c^2/v_A^2 & c^2/v_A^2 \end{pmatrix}. \tag{2b}$$

$v_A^2 = B^2/4\pi\rho$, L is the 2×2 operator

$$L = \begin{pmatrix} -r^{-2}\partial_\theta^2 - \partial_z^2 & r^{-2}\partial_\theta(\partial_r r)\cos a \\ & -\partial_r\partial_z \sin a \\ \cos a\partial_r(r^{-1}\partial_\theta) & -\cos a(\partial_r(r^{-1}\partial_r r) + \partial_z^2)\cos a \\ -\sin a r^{-1}\partial_r(r\partial_z) & -\sin a(r^{-1}(\partial_r r\partial_r) + r^{-2}\partial_\theta^2)\sin a \\ & -\cos a r^{-1}\partial_\theta\partial_z \sin a \\ & -\sin a r^{-1}\partial_\theta\partial_z \cos a \end{pmatrix} \tag{3}$$

and a is the shear angle

$$a(r,\theta) = r/Rq = \epsilon/q(1 + \epsilon\cos\theta) \tag{4}$$

with $\epsilon = r/R_0$ the inverse aspect ratio, $q \equiv q(\psi)$ the safety factor and $\psi(r,\theta)$ the poloidal flux function. L and K are expanded in powers of ϵ

$$L = L_0(r) + \sum_{n=1}^{\infty} \epsilon^{n+1} L_n(r,\theta) \tag{5a}$$

$$K = K_0(r) + \sum_{n=1}^{\infty} \epsilon^n K_n(r,\theta) \tag{5b}$$

where L_0 and K_0 express the cylindrically symmetric θ-independent parts.

$$L_0 = \begin{pmatrix} -\partial_{\|}^2 - \partial_{\perp}^2 & \partial_{\perp}\left[r^{-1}\partial_r r\right] - Z \\ \partial_r \partial_{\perp} + Z & -r^{-1}\partial_r(r\partial_r) - \partial_{\|}^2 + W \end{pmatrix} \tag{6a}$$

with

$$\begin{aligned} \partial_{\perp} &\equiv \cos a_0(r)\frac{1}{r}\partial_{\theta} - \sin a_0(r)\partial_z \\ \partial_{\|} &\equiv \sin a_0(r)\frac{1}{r}\partial_{\theta} + \cos a_0(r)\partial_z \\ Z &= \left(\frac{\partial a_0}{\partial r}\right)\partial_{\|} - \frac{\sin a_0}{r}\partial_z \\ W &= \left(\frac{\partial a_0}{\partial r}\right)^2. \end{aligned} \tag{6b}$$

It is worth noting that the poloidal angle θ enters the metric elements in operator L through the small shear angle $a = \epsilon/q$ Eq. (4) thus for $(\partial/\partial\theta)\ell n\psi \sim O(\epsilon)$ the poloidal corrections enter L to order ϵ^2, Eq. (5a). The higher order terms in the expansions will be derived in Sec. V. However, the formal expressions (5) combined with (6) are sufficient to develop the perturbation techniques of Sec. IV.

The zeroth order equation

$$\left(L_0 - (\omega^2/c^2)K_0\right)\chi = 0, \tag{7}$$

recast in the more familiar form

$$\left[\frac{d}{dr}\frac{F}{r[F - k_{\perp}^2]}\frac{d}{dr}r\right]E_{\perp} + (F+g)E_{\perp} = 0,$$

where

$$F = \left[1 - \frac{\omega^2}{\Omega_i^2}\right]^{-1}\left\{\frac{\omega^2}{v_A^2} - k_{\|}^2\right\}, \tag{8}$$

describes the MHD wave propagation in a current-carrying cylindrical plasma with sheared magnetic field. The solutions of Eq. (8) have been studied extensively due to their fundamental role in determining plasma stability and confinement and their behavior is quite

well understood both analytically and numerically. The toroidal eigenmodes χ, solutions of Eq. (2) can in principle be obtained using perturbation techniques and starting from the cylindrical solutions along with the expansions Eqs. (5). However, the usual calculation, by means of solving differential equations to increasing order in ϵ by iteration, gets immediately complicated by the large number of terms resulting from the convolution between different spectral components of χ, L and K. On the other hand, if certain properties are satisfied by the cylindrical set of solutions, such as orthogonality and completeness, then the toroidal modes can be expressed as a linear superposition of cylindrical modes with the expansion coefficients determined by evaluating the integral projections of the *known* cylindrical modes in respect to some weighting matrix determined by the perturbation. This method avoids direct integration of Eq. (2) and is the MHD analog of the perturbation techniques applied successfully in quantum-mechanical eigenvalue problems.

III. Symmetry and Orthogonality Properties in Cylindrical Geometry

The set of eigenmodes of Eq. (6) can be divided into three classes according to the associated eigenvalue spectrum $\omega^2(k_r, m, n)$ where m is the poloidal and n the toroidal wave number ($k_z = n/R_0$, R_0 major radius of the torus): (a) Unstable discrete usually associated with unstable kink modes with $\omega^2 < 0$ (b) Stable discrete or global Alfvén modes $0 < \omega^2 < \omega^2_{\min}$ (c) Stable Alfvén continuum $\omega^2_{\min} < \omega^2 < \omega^2_{\min}$. Within the first two classes of modes for given m and n there is only a discrete set of radial wave-numbers k_r compatible with the boundary conditions allowing a discrete set of frequencies. The continuum property of the third class implies that for given m and n there is a continuous succession of k_r's and ω's with the position r_0 of the associated resonant layer satisfying the relation

$$\omega^2 = \omega_A^2(r_0, m, n) \equiv v_A^2(r_0) R_0^{-2} (n + m/q)^2.$$

On the other hand, for a given ω^2 there are more than one resonant surfaces $r_0(m, n)$ corresponding to modes with different helicities but the same Alfvén frequency, i.e. (Fig. 2)

$$v_A^2(r_0) R_0^{-2} (n + m/q)^2 = v_A^2(r_0') R_0^{-2} (n' + m'/q')^2 \tag{9}$$

implying that there is natural degeneracy among the continuum eigenmodes (while in the discrete regime of the spectrum degeneracy can only be accidental).

A technical difficulty arises in treating the continuum part of the spectrum due to the logarithmic singularity exhibited by the solution in the vicinity of the resonant layer $r = r_0$ (i.e. $F = 0$). The eigenmodes are non-square – integrable functions, "distributions" of the type investigated by Van Kampen[16] for the case of electrostatic modes. A convergent superposition of these singular modes is all that matters for physical applications provided that a prescription allowing integration is found. Barston[5] used this method to demonstrate the collisionless damping of macroscopic MHD oscillations in the continuum while Tataronis[7,8] and Grossman showed the logarithmic increase in time of the energy

content around a resonant layer externally driven by a frequency matching its local Alfvén frequency.

To avoid heavy formalism we introduce a small imaginary part in the frequency owing to a small anti-Hermitian part in the dielectric tensor

$$K = K^H + \gamma K^A, \quad \gamma << 1$$

caused for example by electron Landau damping. The eigenmodes of the equation

$$\left\{ L_0 - \frac{(\omega_0 + i\gamma)^2}{c^2} \left(K_0^H + \gamma K_0^A \right) \right\} u = 0 \tag{10}$$

are well behaved everywhere on the real axis and square-integrable. The frequency spectrum is discretized, however, by letting $\gamma \to 0$, $|\delta\omega^2|$ for nearby modes can be made arbitrarily small, much less than the size of the toroidal perturbation $O(\epsilon)$ or the spectral width of the exciting antenna.

Now we proceed to show that under general boundary conditions the continuum modes constitute a normalizable ($\gamma \neq 0$), nearly orthogonal set of eigenmodes approaching the ideal δ-function like solutions as $\gamma \to 0$. The inner product between two modes is defined relative to the Hermitian part (K_0^H) of K_0

$$\langle u|v\rangle = \int_V u^* \cdot K_0^H \cdot v \; d^3x \tag{11}$$

and the normalization

$$u_0(\omega^2, \vec{k}; \gamma) = u(\omega^2, \vec{k}; \gamma) / \langle u|u\rangle^{1/2}$$

with

$$u = \begin{pmatrix} E_r(r) \\ E_\perp(r) \end{pmatrix} e^{i\left(m\theta + n/R_0 z\right)}, \quad \vec{k} = (m, n) \tag{12}$$

the subscript (0) being used for the cylindrical modes. From Eqs. (11)-(12) the orthogonality between modes with different $\vec{k}$ is trivial. It remains to be proved for $m = m'$,

$n = n'$ but $\omega_0^2 \neq \omega_0'^2$. It is shown in Appendix A, that the sufficient and necessary condition for exact orthogonality between the solutions of Eq. (10) is that the operator L_0 be symmetric

$$\int_V d^3x \left[u^* \cdot L_0 \cdot v - v \cdot L_0^* \cdot u^* \right] = 0, \tag{13a}$$

provided that the weighting matrix K_0 is Hermitian

$$K_0 = K_0^+ \equiv (\tilde{K}_0)^*. \tag{13b}$$

The symmetry condition Eq. (13) holds under general boundary conditions given by Eq. (A6), which include perfectly conducting boundaries. A small departure from orthogonality is left from the small anti-Hermitian part in K_0.

$$\langle u(\omega^2, \vec{k}) | u(\omega'^2, \vec{k}) \rangle = \delta_{mm'} \delta_{nn'} \left\{ \delta(\omega_0^2 - \omega_0'^2) + 0(\gamma) \left[1 - \delta(\omega_0^2 - \omega_0'^2) \right] \right\}. \tag{14}$$

Thus if the solutions of Eq. (10) are conceived as vectors in Hilbert space, the effect of γ is to introduce a small departure from mutual orthogonality that disappears with $\gamma \to 0$.

We assume completeness without proving it. However, we do feel that since completeness can be proved for the Bessel functions solutions for a uniform plasma, an adiabatic change to a non-uniform plasma would not alter the situation as long as we include all the new modes introduced by the inhomogeneity.

IV. Toroidal Alfvén Modes as Superposition of Cylindrical Eigenmodes

By letting γ become smaller than ϵ, $\epsilon^2 \ldots \epsilon^n$ the quantities related to γ can be neglected and the expansion coefficients can be obtained to order ϵ^n by applying perturbation theory to the equation

$$\left[L - \frac{\omega^2}{c^2} K^H \right] \chi = 0, \tag{15}$$

from now on, dropping the superscript (H) unless otherwise indicated. The expansions Eqs. (3) are used for L and K while χ and ω^2 are expanded according to

$$\chi(\omega^2) = \sum_{\omega_0, m'} \left\{ \sum_{\ell=0}^{N} \epsilon^\ell g_\ell(\omega_0^2, m') \right\} u_0(\omega_0^2, m'; \gamma) \tag{16a}$$

$$\omega^2 = \omega_0^2 + \sum_{\ell=1}^{N} \epsilon^\ell h_\ell. \tag{16b}$$

The perturbation $K - K_0$ is axisymmetric and does not mix modes with different toroidal wave numbers; n is kept fixed and from now on it will be suppressed as an index.

For perturbed modes with $\omega^2 \simeq \omega_0^2$ in the continuum, degenerate perturbation technique must be applied within the subset of the N degenerate eigenmodes $\omega_0^2(m_i, n) = \omega_0^2$, $i = 1, \ldots, N$ contained among the full set of solutions of Eq. (10). This subset includes modes in the continuum plus these modes in the discrete part of the spectrum with frequencies ω_D^2 in the regime $|\omega_D^2 - \omega_0^2|/\omega_0^2 << \epsilon$. The same treatment must be applied for the almost degenerate modes located within the narrow band $|\omega^2 - \omega_0^2(m_i, n)| < \omega^2 \Delta$, $\Delta << \epsilon$ for each branch $\omega^2(m_i, n)$ of the continuum (see Fig. 2). We assume that the number of the exactly degenerate modes is finite by keeping finite density everywhere between the boundaries and expand χ and ω^2 to first order in ϵ

$$\chi(\omega^2) = \sum_{i=1}^{N} \int_{\omega_0^2(1-\Delta)}^{\omega_0^2(1+\Delta)} g_0(\bar{\omega}^2, m_i) u_0(\bar{\omega}^2, m_i) d\bar{\omega}^2$$
$$+ \epsilon \sum_{m'} \left[\sum_{\bar{\omega}^2 > \omega_0^2(1+\Delta)} + \sum_{\bar{\omega}^2 < \omega_0^2(1-\Delta)} \right] g_1(\bar{\omega}^2, m') u_0(\bar{\omega}^2, m') \tag{17a}$$

$$\omega^2 = \omega_0^2 + \epsilon h_1. \tag{17b}$$

In case that $u_0(\bar{\omega}^2, m_i)$ corresponds to degeneracy involving a discrete mode $g_0(\bar{\omega}^2, m_i)$ is simply given by $\delta[\bar{\omega}^2 - \omega_D^2(m_i)] g_0(\omega_D^2, m_i)$. The inclusion of finite bandwidth around the degenerate modes in the continuum leads to the following system of integral equations for the determination of the coefficients g and h

$$h_1 g_0(\varsigma, m_i) = -\sum_{j=1}^{N} \int_{\omega_0^2(1-\Delta)}^{\omega_0^2(1+\Delta)} d\bar{\varsigma} \langle u_0(\varsigma, m_i) | \omega_0^2 K_1 | u_0(\bar{\varsigma}, m_j) \rangle g_0(\bar{\varsigma}, m_j)$$

where $\varsigma = \omega^2$. From Eqs. (25) (in next section) with $n = 1$, one sees that $K_1 = K_0 + 0(\omega/\Omega_0) \begin{pmatrix} 0 & i \\ -i & 0 \end{pmatrix}$ thus the inner product in the r.h.s. of the above equation is peaked

around $\varsigma = \bar{\varsigma}$ and can be approximated by

$$\langle u_0(\varsigma, m_i)|\varsigma K_1|u_0(\varsigma, m_j)\rangle \delta(\varsigma - \bar{\varsigma}).$$

We may set $\varsigma = \varsigma_0 = \omega_0^2$ utilizing the slow variation of the matrix element in ω^2 leading to the uniform system with constant coefficients U_{ij}

$$\begin{aligned} h_1 g_0(m_i) &= \sum_j U_{ij} g_0(m_j) \\ U_{ij} &= -\omega_0^2 \int_V d^3x \; u_0^*(\omega_0^2, m_i) \cdot K_i \cdot u_0(\omega_0^2, m_j). \end{aligned} \tag{18}$$

The solutions $g_0(m_i)$ are determined with a multiplication constant to be found either by normalization or boundary conditions, while h_1 is one of the eigenvalues λ of the characteristic equation

$$\det\|U - \lambda I\| = 0. \tag{19}$$

In general, there are N real eigenvalues $h_1^{(k)}$, $k = 1, ..., N$ as K_1 is Hermitian with N associated expansion coefficients vectors $\vec{g}_0^{(k)} \equiv \big(g_0(m_1) \ldots g_0(m_N)\big)^{(k)}$. The diagonalization of the matrix U is particularly easy in case when K_1 has only one spectral component $K_1 \cos\theta = \frac{1}{2} K_1 (e^{i\theta} + e^{-i\theta})$ as this yields the tridiagonal matrix

$$(U - \lambda I)_{ij} = \delta_{i,j+1} \bar{U}_{ij} - \delta_{ij}\lambda + \delta_{i,j-1} \bar{U}_{ij}$$

with

$$2\bar{U}_{ij} = -\omega_0^2 \int_a^b dr \; r \; u_0^*(\omega_0^2, m_i) \cdot K_1 \cdot u_0(\omega_0^2, m_j).$$

Equation (17a) is written to zeroth order as

$$\chi^{(k)}(\omega^2) = \sum_i g_0^{(k)}(m_i) \bar{u}_0(\omega_0^2, m_i) \tag{20}$$

where $\bar{u}_0(\omega_0^2, m_i) \equiv \int_{\omega_0^2(1-\Delta)}^{\omega_0^2(1+\Delta)} d\bar{\omega}^2 u_0(\bar{\omega}^2, m_i)$ are the cylindrical modes with some broadening in the width of the resonant layer. Thus, owing to the degeneracy, toroidicity produces a

large change in the radial profiles resulting from the zeroth order mixing between cylindrical modes, while the correction in the frequency ω^2 remains small of order ϵ. The toroidal modes exhibit many discrete resonant surfaces associated with different helicity m but the same local Alfvén frequency $\omega_A^2(m,n)$. As each term u_0 in the expansion Eq. (20) is localized within a width $|\delta r/r_0| << \epsilon$ around its own resonant layer $r_0(m,n)$, the resonant surfaces retain their generic poloidal dependence and cylindrical shape. This should not be surprising as the toroidal effects in operator L have not been considered yet, entering to order ϵ^2. For ω^2 held fixed the position of each resonant layer is shifted relative to its generic position r_0 given by $v_A^2(r_0) = \omega_0^2/k_\parallel^2$ as from Eq. (17b)

$$v_A^2(r) = \left[\omega^2 - \epsilon h_1^{(k)}\right]/k_\parallel^2.$$

The contributions from terms with $\omega_0'^2 \neq \omega_0^2$ entering to order ϵ in χ and ϵ^2 in ω^2 is further diminished by the phase mixing among large numbers of different radial profiles.

The old degeneracy between cylindrical modes is broken as to each of the coefficient vectors $\vec{g}_0^{(k)}$ corresponds to a different $\omega^{2(k)} = \omega_0^2 + \epsilon h_1^{(k)}$. However a new degeneracy appears between toroidal modes as follows: one of the new frequencies $\omega^{2(k)} = \omega_0^2 + \epsilon h_1^{(k)}$ may be equal to one of the frequencies produced by the mixing of cylindrical modes with $\bar{\omega}_0^2$ close to but different than ω_0^2 according to

$$\omega_0^2 + \epsilon h_1^{(k)} = \bar{\omega}_0^2 + \epsilon \bar{h}_1^{(\ell)}.$$

The degeneracy between cylindrical modes of the same helicity $\omega_0^2(m,n) = \omega_0^2(-m,-n)$ still remains as the perturbation does not couple modes with different toroidal numbers n. A particular case of degeneracy is encountered[17] when Eq. (9) is satisfied by two different helicity modes with the same resonant layer position r_0 : $(m+n/q)^2 = (m'+n'/q)^2$. This situation, arising due to two *intersecting* branches of the continuum leads to a gap formation in the spectrum ω_0^2 around the intersection point. Since $n = n'$ for coupling, we must have $m + m' = -2n/q$, thus in case of large n and q around unity it takes a high spectral component in the perturbation K_1 to couple m with m'.

Because degeneracy, degeneracy breaking and gap formation is a common phenomenon in systems with one or more degrees of periodicity, it is useful to put the Alfvén wave degeneracy in perspective with some rather familiar examples. One for instance may consider the quantum mechanical textbook example of the energy spectrum of an electron in a one-dimensional periodic potential with period L. There is double degeneracy between the two branches $\omega(k)$ of the free electron energy $E(k) = \hbar\omega = \frac{\hbar k^2}{2m}$ as for every k $\omega(k) = \omega(-k)$, Fig. 3. Now, if the periodic potential $V(x) = \sum_{n=-\infty}^{\infty} V_n e^{inQx}$, $Q = \frac{2\pi}{L}$, is introduced as a perturbation, it will couple unperturbed states with k's satisfying $k_1 - k_2 = nQ$. Of all the degenerate pairs of frequencies only these corresponding to $k = \pm\frac{n}{2}Q$ will be strongly coupled leading to gap formation while the degeneracy still remains. Now let us consider the degenerate Alfvén spectrum $\omega^2 = k_{||}^2(r)v_A^2(r) = v_A^2(r)R_0^{-2}[m^2 + n^2/g^2(r)]$ plotting ω^2 as a function of q. For simplicity we consider only three non-intersecting branches with m_1, m_2 and m_3 keeping n fixed. The mirror image curves on the left-hand side of Fig. 4 (dots) correspond to the degeneracy $\omega^2(k_{||}) = \omega^2(-k_{||})$. These branches $\omega^2(-k_{||}) \equiv \omega^2(-m, -n)$ cannot couple to the right-hand side branches $\omega^2(k_{||}) \equiv \omega^2(m, n)$ through a toroidally symmetric perturbation $K_M(r)\left[e^{im\theta} + e^{-im\theta}\right]$ that does not mix states with different n. (This coupling however could be achieved by a helical perturbation $K_{M,N}e^{iM\theta+iN\phi}$ with $m = \pm\frac{M}{2}$, $n = \pm\frac{N}{2}$ resulting in gap formation as in Fig. 3). Instead any three cylindrical states defined by the intersection of the line $\omega_0^2 =$ constant with the branches $m_1 = m_0 - M$, $m_2 = m_0$, $m_3 = m_0 + M$ are strongly coupled by K_M. Contrary to the situation in Fig. 3 where the coupling is effective for special values of $\omega(k)$, these with $k = \pm nQ/2$, in the Alfvén wave case one can draw the line $\omega^2 =$ constant that defines the degeneracy from any point in Fig. 4. The coupling condition with the perturbation $m_i \pm m_j = M$ is independent of q and satisfied everywhere along the considered branches m_1, m_2, m_3. Therefore the effect of toroidicity is not localized in a particular part of the spectrum (as in the gap formation case) but is global.

Let $\Omega_1^2 = \omega^2 + \epsilon\delta_1(\omega^2)$, $\omega_2^2 = \omega^2 + \epsilon\delta_2(\omega^2)$, $\Omega_3^2 = \omega^2 + \epsilon\delta_3(\omega^2)$ with δ_i the eigenvalues

λ of Eq. (19) be the new frequencies produced by the mixing of cylindrical modes of frequency ω^2. The new dispersion branches are drawn by shifting all the unperturbed branches by the same $\epsilon\delta_i(\omega^2)$ for each Ω_i^2 $i = 1,2,3$ as shown in Fig. 5. All segments marked by the same label i now correspond to one toroidal branch of the dispersion relation and a single mode of frequency Ω_i^2 is associated with all three poloidal numbers m_1, m_2, m_3 or equivalently three different $k_{||}$. A single frequency mode has also many resonant surfaces $q_r(m)$ that are shifted relative to their position in a cylinder as seen by taking the projections of the intersection points of the line $\Omega^2 =$ constant with the different segments of the curve $\Omega_i^2(q)$ onto the q axis. It is also obvious from Fig. 5 that a given m and a given q (equivalent to given $k_{||}$ and r) does not uniquely determine the toroidal mode frequency Ω^2 as it would do in the cylindrical case; m is not a "good" quantum number in toroidal geometry. The functions $\delta_i(\omega^2)$ are continuous functions of ω^2 as roots of the polynomial Eq. (19). Therefore it is proved that a new degenerate continuum of toroidal eigenmodes exists in place of the old degenerate continuum of cylindrical modes.

So far gaps have not appeared in our analysis. They come into play in the special case when intersecting branches in the cylindrical dispersion relation are considered. The two unperturbed modes with frequency ω^2 near the intersection regime of curves 1 and 2 (Fig. 6(a)) have the same resonant position q. They must satisfy $m_1 + m_2 = -2n/q$ because they must have the same $k_{||}$ and $m_1 - m_2 = M$ to couple through the perturbation. The condition $M = 2m_1 + 2n/q$ with $2n/q$ integer must be valid for this special regime of the spectrum, examined in detail in Ref. 17. In this case an additional ordering must be taken into account: the overlapping between the modes around the intersection is very strong because their wavefunctions are localized around the same resonant surface. The coupling coefficients U_{ij} between the modes 1 and 2 in Eq. (18) are much larger than these between 3 and 1 or 3 and 2 resulting into much larger frequency correction $G(\omega^2)$ compared to $\delta(\omega^2)$ caused by non-intersecting branches. That suggests carrying the diagonalization of the degenerate subspace in two steps. First we diagonalize around the intersection point

the intersection point ignoring all other branches to obtain the gap in the continuum[17] $G(\omega^2)$, Fig. 6(a). In a second step we resolve the remaining degeneracy between the modified branches 1, 2 and remaining branch 3 (or any more remaining branches for that matter). During the second diagonalization and for frequencies falling into the gap regime degeneracy can exist only between different non-intersecting branches. Therefore, the number of toroidal modes with given frequency ω^2 within $G(\omega^2)$ equals the number of the unperturbed non-intersecting branches (only one in Fig. 6(b)). Outside the gap we again have three interacting branches with the new frequency corrections causing a modification of the gap with $G'(\omega^2) = G(\omega^2) - \delta_1(\omega^2) - \delta_2(\omega^2) - \delta_3(\omega^2)$.

V. Higher Order Expansions

We now proceed to consider the role of toroidicity in the operator L by carrying the perturbation to a higher order in ϵ. The shear angle $a(r,\theta)$, Eq. (4), is expanded in powers of ϵ assuming that the flux profile and g are given by

$$\psi(r,\theta) = \psi_0(r) + \psi_1(r)\epsilon\cos\theta q(r,\theta) = A\psi + B. \tag{21}$$

We set $\epsilon\cos\theta = \mu$, utilize the property $\partial^n/\partial\mu^n(1/q) = q_0^{-(n+1)}(\partial q/\partial\mu)^n$ due to (18), and expand $\cos^n\theta$ in harmonics to obtain after some algebra

$$a(r,\theta) = a_0(r) + \delta a(r,\theta) \tag{22a}$$

with

$$a_0(r) = \epsilon/q_0, \quad q_0(r) = A\psi_0(r) + B$$
$$\delta a(r,\theta) = \sum_{n=1}^{\infty} a_n(r)\cos n\theta, \tag{22b}$$

$$a_n(r) = \left(\frac{\epsilon}{q_0}\right)(-1)^n\left(\frac{\epsilon}{2}\right)^n\left[\left(\frac{A\psi_1(r)}{q_0}\right) + 2\right] \tag{22c}$$

where only the leading order contribution was kept in each Fourier coefficient $a_n(r)$. A first order expansion of Eq. (3) in δa given by Eq. (22) yields after some lengthy but straightforward calculation the spectral decomposition of the operator L

$$L = L_0 + \sum_{n=1}^{\infty}\epsilon^{n+1}\left\{e^{in\theta}L_n^+ + e^{-in\theta}L_n^-\right\} \tag{23a}$$

with

$$L_n^{\pm} = \begin{pmatrix} 0 & -c_n\partial_{\|}[r^{-1}\partial_r r] \\ & -(\partial_r c_n)\cos a_0\partial_z \\ -\partial_r(c_n\partial_{\|}) + \partial_r & \pm inr^{-1}c_n\cos\ 2a_0\partial_z \\ +(\partial_r c_n)\cos a_0\partial_z & \end{pmatrix} \tag{23b}$$

and

$$c_n(r) = 2^{-n}\big(1/q_0(r)\big)\big[\big(A\psi_1(r)/q_0(r)\big) + 2\big]. \tag{23c}$$

The expression of the dielectric tensor K by setting

$$B^2 = B_0^2R_0^{-2}(1+\epsilon\cos\theta)^{-2}$$
$$\rho(\psi) = D\big[\psi_0(r) + \psi_1(r)\epsilon\cos\theta\big] + E \tag{24}$$

yields in a similar manner

$$K = K_0 + \sum_{n=1}^{\infty} \epsilon^n K_n \frac{1}{2}\left(e^{in\theta} + e^{in\theta}\right) \tag{25a}$$

where

$$K_n = \begin{pmatrix} f_n\, v_{0A}^2/c^2 & -i\tilde{f}_n\, \omega/\Omega_0\, v_{0A}^2/c^2 \\ i\tilde{f}_n\, \omega/\Omega_0\, v_{0A}^2/c^2 & f_n\, v_{0A}^2/c^2 \end{pmatrix} \tag{25b}$$

and

$$\begin{aligned} f_n &= (-1)^n 2^{-n}\left[2n + (n-1)(D\psi_1(r)/\rho_0)\right] \\ \tilde{f}_n &= (-1)^n 2^{-n}\left[2 + (D\psi_1(r)/\rho_0)\right]. \end{aligned} \tag{25c}$$

Equation (23a) has the nice feature that the higher Fourier components are ordered in ascenting powers of ϵ. As on the leading order contribution in ϵ was considered in each term of the sum, it can be shown that expression (23c) is invariant to the use of more general expressions $\psi(r, \epsilon\cos\theta)$ in place of (21). The most important property however is that Eq. (23) preserves the original symmetry of the operator L to all orders in ϵ; this was proved for L_0 and it can be shown directly term by term that

$$\int_V d^3x\left[u^* \cdot L_n^+ \cdot v - v \cdot (L_n^-)^* \cdot u^*\right] = 0$$

under the same boundary conditions. The Hermiticity of K^H is also preserved by the expansion (25).

The symmetry property is utilized by showing that the eigenfunctions u of the equation

$$Lu - \frac{(\omega_0 + i\gamma)^2}{c^2}\left(K_0^H + \gamma K_0^A\right)u = 0 \tag{26}$$

form an almost orthogonal set of functions, using the same procedure as in Sec. III. Assuming that the solutions u of the above equation are found, it suffices to consider the toroidicity effects in the dielectric matrix K alone to carry out the perturbation theory.

First we obtain the toroidal eigenmodes u in the form of a power series in ϵ. Introducing the ansätz

$$u(\omega, m, n) = \left\{u^{(0)} + \sum_{k=1}^{\infty} \epsilon^{k+1}\left[u_+^{(k)} e^{-ik\theta} + u_-^{(k)} e^{ik\theta}\right]\right\} e^{i(m\theta + n/Rz)}, \tag{27}$$

expanding L according to Eq. (4a) and ordering in ϵ we obtain the following hierarchy of equations for the components $u_{\pm}^{(k)}$

$$(L_0 - \frac{\omega^2}{c^2}K_0)u^{(0)} = 0 \tag{28a}$$

$$(L_0 - \frac{\omega^2}{c^2}K_0)u_{\pm}^{(1)} = -L_1^{\mp}u^{(0)} \tag{28b}$$

$$\vdots \qquad \vdots$$

$$(L_0 - \frac{\omega^2}{c^2}K_0)u_{\pm}^{(k)} = -\sum_{\ell=1}^{k} L_{\ell}^{\mp}u^{(k-\ell)}. \tag{28c}$$

The above system can be solved recursively, as each term on the l.h.s. is driven by lower order terms on the r.h.s. The first equation immediately yields

$$u^{(0)} \equiv u_0(\omega_0^2, m, u). \tag{29}$$

The $u_{\pm}^{(1)}$ term in the second equation is driven by the $u^{(0)}$ source term in the r.h.s. Since $u^{(0)} \equiv u_0$ is localized around its generic resonant surface, an $m \mp 1$ poloidal dependence appears to order ϵ^2 around the m-cylindrical resonant surface, according to Eqs. (28). By inspection of the rest of the equations, it is verified that an $m \pm k$ spectral component appears around the m-cylindrical resonant surface to order ϵ^{k+1}. The formal solution of the general case Eq. (28c) is given by

$$u_{\pm}^{(k)}(r) = -\sum_{\ell=1}^{k}\int_a^b dr' G(r', r)L_{\ell}^{\mp}u^{(k-\ell)}(r') + \sigma_1 S_1(r) + \sigma_2 S_2(r) \tag{30}$$

where $G(r, r')$ is the Green's function constructed by the two linearly independent solutions $S_1(r)$ and $S_2(r)$ of the *uniform* Eq. (28a) and σ_1, σ_2 are constants to be determined by the boundary conditions at a and b. The toroidal modes $u(\omega_0^2, m, n)$ are non-monochromatic in θ, with m now signifying the *zeroth* order poloidal dependence, but they are still radially localized close to the resonant layer of the cylindrical mode $u_0(\omega_0^2, m, n)$. Defining the new resonant surface at the radial maximum of $|u(r, \theta)|$ we obtain using Eq. (27) a relation

$$f(r, \theta) = \frac{\partial u}{\partial r} = 0$$

expressing a generally non-circular cross-section.

The toroidal corrections in K_0 are added in the r.h.s. of Eq. (25) and the perturbation theory is worked out using the χ and ω^2 expansions, Eqs. (16a) and (16b) of Sec. IV, with the cylindrical modes $u_0(\omega_0^2, m, n)$ replaced by the "toroidal" modes $u(\omega_0^2, m, n)$. Although $u(\omega_0^2, m, n)$ are in themselves asymptotic series in ϵ, it is to our advantage to formally treat the series as one function utilizing their mutual orthogonality in respect to the weighting matrix K_0. After obtaining the expansion coefficients, the representation for u's can be truncated to the desired accuracy. It is immediately justifiable that a first order truncation reproduces the results in Eqs. (17).

VI. Discussion and Summary

The toroidal Alfvén modes have been constructed by a superposition of cylindrical eigenmodes with the development of a perturbation technique for the determination of the expansion coefficients.

The procedure is shown schematically in Figs. 7(a)-(d) where for simplicity only three modes $m-1$, m and $m+1$ are considered. In (a) the typical radial profile $E_\perp(r)$ for each cylindrical mode $u_0(\omega_0^2, m)$ is shown localized around one resonant surface. The modifications due to the toroidicity effects in L lead to the non-monochromatic modes $u(\omega_0^2, m)$ solutions of Eqs. (27) and (28) shown in Fig. 7(b). Different helicity contributions appear on each resonant surface on top of its generic poloidal dependence. The toroidal modes $\chi(\omega^2)$ in Fig. 7(c) show the mixing between different resonant surfaces produced by the perturbation in the dielectric tensor K_1. In general, three different linear combinations of $u(\omega_0^2, m)$, $u(\omega_0^2, m \pm 1)$ exist producing three different toroidal modes $\chi(\omega^2)$. The resonant surfaces are shifted from their generic positions. In Fig. 7(d) the higher order terms are dropped from Fig. 7(c). These approximate solutions are produced by the mixing of the purely cylindrical modes of Fig. 7(a) and are obtained immediately from the lower order perturbation theory Eqs. (18)-(20).

For practical purposes (small ϵ) the zeroth order expansion coefficients $\vec{g}_0^{(k)}(m_i)$ and the first order correction in frequency $h_1^{(k)}$ may provide a sufficient account for the local energy absorption around the (m_i, n) resonant layer. More specifically, the local energy absorption is associated with the discontinuity of the Poynting flux vector near the (m_i, n) resonant layer and is determined merely by the structure of the $u_0(\omega_0^2, m_i, n)$ mode near this layer. In the dimensionless variable $x = (r - r_0)/w$, the distance from the resonant surface scaled to the local resonant width $w = \left[\frac{d}{dr}\left(K_0(r)\frac{\omega^2}{c^2} - k_\parallel^2(r)\right)\right]^{-1/3}_{r=r_0}$, each cylindrical mode behaves in the vicinity of its resonant layer as

$$E_\perp(\omega_0^2, m_i, n) \simeq c_1 K_0(x) + c_2 I_0(x). \tag{31}$$

(Note that with $\omega_0 \to \omega_0 + i\gamma$ r_0 defined by $v_A^2(r_0) = \omega_0^2/k_\parallel^2$ picks an imaginary part $r_0 \to r_0 + i\xi$ that prevents $K_0(x) \sim \ell n\ x$ from blowing up at $\mathrm{Re}(x) = 0$.) The absorption coefficient associated with Eq. (31) is[19,20]

$$\Gamma = \frac{2\pi}{\sqrt{3}} w^2 \left[k_\perp(r_0)\left(\frac{c_2}{c_1}\right)^{1/2} - \left(\frac{\omega}{\Omega_i} k_\parallel^2(r_0) + \kappa^2(r_0)\right) w \left(\frac{c_1}{c_2}\right)^{1/2} \right]^2 \tag{32}$$

with $c_1 = Ai(0) = .355$, $c_2 = Ai'(0) = .259$ and $\kappa(r_0) = (1/w)(da/dr)$, with $a(r)$ the shear angle. The above formula includes the effects of both finite frequency ω/Ω_i and finite shear κ. The absorption coefficient for the ideal MHD Alfvén resonance without shear is obtained by setting ω/Ω_i and κ equal to zero. When either ω/Ω_i or κ are finite, the absorption is modified by the appearance of a cutoff-resonance-cutoff triplet and for certain parameter combinations Eq. (32) describes a mild damping of excited cavity modes,[18,19,20] $\Gamma << 1$. As the portion of the θ-averaged energy flux carried by each cylindrical component contributing in the expansion Eq. (20) is proportional to $|g_0(m_i, n)|^2$, the local absorption coefficient for the toroidal mode $\chi(\omega_0^2)$ at the surface $r_0(m_i, n)$ is

$$\Gamma_0 |g_0(m_i, n)|^2 \Gamma(m_i, n) \tag{33}$$

with the constant Γ_0 to be determined from the matching conditions with the antenna.

Numerical results showing qualitative behavior in agreement with our theory are described in Refs. 21-22. In particular, the numerical results for the excitation of toroidal plasmas by a single helicity antenna show (a) excitation of all the different helicity resonant surfaces resonating with the antenna to about the same order (b) shift of the resonant surfaces relative to their position in a cylinder (c) presence of the other spectral components scaling as powers of ϵ on top of a resonant surface with given m and (d) significant power absorption appearing as a step-like reduction in the incoming Poynting flux level in the vicinity of resonant layers located on the outside of the intended, matching the antenna helicity, resonant layer. Quantitative agreement should not be expected however as the imaginary part in the frequency, imposed for numerical reasons in the above simulations, was comparatively large $\gamma/\omega_0 \sim 0(\epsilon)$ resulting in a considerable violation of the orthogonality condition, Eq. (14).

Our method should be particularly applicable in determining the destabilization of the marginally stable $\omega_0^2 \simeq 0$ ideal kink modes due to toroidal effects and thus the modification of the MHD stability boundary against the nonlocalized external kink modes. The method would be complementary to the Mercier stability analysis,[25] the toroidal extension of the cylindrical stability theory, that applies for the case of localized internal modes and yields a necessary (but not sufficient) stability criterion. This regime of application also offers freedom from mathematical singularities.

Appendix A: Proof of Symmetry and Orthogonality

We present here a more detailed analysis of the symmetry and orthogonality properties for the cylindrical MHD eigenmodes introduced in Sec. III. We start with Eq. (10)

$$(L_0 + \frac{\omega_u^2}{c^2} K_0)u = 0 \tag{A1}$$

$$(L_0 + \frac{\omega_v^2}{c^2} K_0)v = 0 \tag{A2}$$

where $\omega_u = \omega_{01} + i\gamma\delta\omega_1$, $\omega_u = \omega_{02} + i\gamma\delta\omega_2$ $K_0 = K_0^H + \gamma K_0^A$, $\gamma << 1$ and

$$u = \begin{pmatrix} X_1 \\ Y_1 \end{pmatrix} e^{2\left(m_1\theta + n_1/R\ z\right)}$$

$$v = \begin{pmatrix} X_2 \\ Y_2 \end{pmatrix} e^{i\left(m_2\theta + n_2/R\ z\right)}$$

$$X \equiv E_r \qquad \text{and} \qquad Y \equiv E_\perp.$$

Multiplying Eq. (A2) with u^*, the complex conjugate of Eq. (A1) with v and subtracting we obtain

$$\int_V (u^* L_0 v - v L_0^* u^*) d^3x = \int_V \left[\frac{\omega_u^2}{c^2} u^* K_0 v - \frac{(\omega_u^*)^2}{c^2} v K_0^* u^*\right] d^3x. \tag{A3}$$

Symmetry is established by proving the existence of a class of boundary conditions for which the l.h.s. of Eq. (A3) vanishes

$$\int_V (u^* L_0 u - u L_0^* u^*) d^3x = 0. \tag{A4}$$

Substituting expression (6a) for L_0 into (A4) we obtain

$$\delta_{m_1 m_2}\delta_{n_1 n_2} \int_a^b dr\ r\Phi(r) = 0 \tag{A5}$$

$$\Phi(r) = i\left\{X_1^* \frac{k_\perp}{r}\partial_r(rY_2) + Y_2\partial_r(k_\perp X_1^*) + X_2\frac{k_\perp}{r}\partial_r(rY_1^*) + Y_1^*\partial_r(k_\perp X_2)\right\}$$
$$+ \left\{Y_1^*\frac{1}{r}\partial_r(r\partial_r)Y_2 - Y_2\frac{1}{r}\partial_r(r\partial_r)Y_1^*\right\}.$$

Integration of (A5) yields

$$\delta_{m_1 m_2}\delta_{n_1 n_2}\left\{r(Y_1^*\partial_r Y_2 - Y_2\partial_r Y_1^*) - ik_\perp r(X_1^* Y_2 + X_2 Y_1^*)\right\}\Big|_a^b = 0.$$

The above relation is trivially satisfied for $m_2 \neq m_2$ or $n_1 \neq n_2$; the case $m_1 = m_2$ and $n_1 = n_2$ is satisfied by the following boundary conditions

$$\begin{aligned} k_\perp r(X_1^* Y_2 + X_2 Y_1^*)\Big|_a^b &= 0 \\ r\left(Y_1^*\frac{\partial Y_2}{\partial r} - Y_2\frac{\partial Y_1^*}{\partial r}\right)\Big|_a^b &= 0 \end{aligned} \qquad (A6)$$

which include perfectly conducting cylindrical boundaries as a special case, $E_\perp(a=0) = E_\perp(b=r_0) = 0$. ($E_\perp$ lies on the $\hat{e}_\theta$, $\hat{e}_z$ plane, Fig. 1).

We now show that the established symmetry property for the operator L_0, Eq. (A4) under the boundary conditions of Eq. (A6), is a sufficient condition for orthogonality when the dielectric matrix K is Hermitian. Equation (A3) yields

$$\left(\omega_v^2 - (\omega_u^*)^2\right)\int_V d^3x\; u^*\cdot K_0^H\cdot v + \gamma\left(\omega_v^2 + (\omega_u^*)^2\right)\int_V d^3x\; u^*\cdot K_0^A\cdot v = 0 \qquad (A7)$$

using the properties $(K_0^H)^* = \tilde{K}_0^H$ and $(K_0^A)^* = -\tilde{K}_0^A$, $\tilde{K}$ meaning the transpose matrix of K. Consider the non-degenerate case first, $|\omega_u^2 - \omega_v^2| >> \gamma$. For $\gamma = 0$ (exact Hermiticity) we obtain from (A7) the orthogonality condition

$$< u|v > \equiv \int_V d^3x\; u^*\cdot K_0^H\cdot v = 0$$

By setting $u \equiv v$ it is further proved that the eigenvalues are real, $\omega_u^2 = (\omega_u^2)$, provided that $u^*\cdot K_0^H\cdot u$ preserves sign in $a \leq r \leq b$. Using the properties of the second degree polynomials one can show that a sufficient (but not necessary) condition for sign preservation is $\det(K_0^H(r)) \geq 0$, $a \leq r \leq b$, clearly valid in the MHD regime with K_0 given by Eq. (2b). For small but finite γ, Eq. (A5) yields the following result

$$\left|\frac{< u|v >}{< u|u >}\right| = |\gamma|\frac{|\omega_v^2 + (\omega_u^*)^2|}{|\omega_v^2 - (\omega_u^*)^2|}\frac{|\int d^3x u^*\cdot K_0^A\cdot v|}{|\int d^3x u^*\cdot K_0^H\cdot v|} \simeq 0(\gamma) << 1, \qquad (A8)$$

thus a small departure from exact Hermiticity results in almost orthogonal eigenfunctions. In case of degeneracy $\omega_u^2 = \omega_v^2$ the orthogonality condition does not result automatically from Eq. (A7) even for γ exactly zero and u, v may or may not be orthogonal. In the second case mutually orthogonal eigenmodes can always be constructed by a linear orthogonalization within the countable degenerate subset (countable branches of the dispersion curves $\omega_A^2(m,n)$).

It is trivial to show that the symmetry property of the operator L_0 is also a necessary condition for orthogonality when K is Hermitian $K \equiv K_0^H$ as the right-hand side of Eq. (A3) becomes zero by definition for mutually orthogonal u and v.

References

1. M.D. Kruskal, J.L. Johnson, M.B. Gottlieb, and L.M. Goldman, Phys. Fluids **1**, 421 (1958).
2. V.D. Shafranov, Sov. Phys. Techn. Phys. **15**, 175 (1970).
3. B.R. Suydam, IAEA Geneva Conf. **31**, 157 (1958).
4. J.A. Wesson, Nucl. Fusion **18**, 87 (1978).
5. E.M. Barston, Annals of Phys. **29**, 282 (1964).
6. Z. Sedlaček, J. Plasma Phys. **5**, 239 (1971).
7. J.A. Tataronis, J. Plasma Phys. **13**, 87 (1975).
8. J.A. Tataronis and W. Grossman, Z. Physik **267**, 203 (1973).
9. X.P. Pao, Nucl. Fusion **15**, 631 (1975).
10. A. Hasegawa and L. Chen, Phys. Rev. Lett. **35**, 370 (1975).
11. A. Hasegawa and L. Chen, Phys. Fluids **19**, 1924 (1976).
12. D.W. Ross, G.L. Chen and S.M. Mahajan, Phys. Fluids **25**, 652 (1982).
13. S.M. Mahajan, D.W. Ross and L.G. Chen, Phys. Fluids **26**, 2195 (1983).
14. S.M. Mahajan, Phys. Fluids **27**, 2238 (1984).
15. C.M. Ryu and R.C. Grimm, J. Plasma Phys. **32**, 207 (1984).
16. N.G. Van Kampen, Physica **21**, 949 (1955).
17. C.E. Kieras and J.A. Tataronis, J. Plasma Phys. **28**, 395 (1982).
18. E. Ott, J. Wersinger and P. Bonoli, Phys. Fluids **21**, 2306 (1978).
19. C. Karney, F. Perkins and Y. Sun, Phys. Rev. Lett. **42**, 1621 (1979).
20. S. Riyopoulos, Ph.D. Thesis, University of Maryland, pg. 72-76 (1983).
21. K. Appert, B. Babet, R. Gruber, F. Troyon, T. Tsunematsu, and J. Vaclavik, in Heating in Toroidal Plasmas (Proc. 2nd Joint Varenna-Grenoble Int. Symp.), ed. by IAEA Brussels, Belgium, Vol. II, 643 (1980).
22. K. Appert, B. Babet, R. Gruber, F. Troyon, T. Tsunematsu, and J. Vaclavik,

Nucl. Fusion **22**, 903 (1982).

23. R.D. Bengtson, T.E. Evans, Y.M. Li, S.M. Mahajan, M.E. Oakes, D.W. Ross, C.M. Surko, P.M. Valanju, X.Z. Wang, and J.G. Watkins, Proc. of the 4th Int. Symp. on Heating in Toroidal Plasma, Roma, ed. by ENEA Varenna, Italy, Vol. 1, 121 (1984).
24. A. de Chambrier, G.A. Collins, P-A. Duperrex, A. Heym, F. Hofmann, Ch. Hollenstein, B. Joye, R. Keller, A. Lietti, J.B. Lister, F.B. Marcus, J-M. Moret, S. Nowak, A. Pochelon, W. Simm, and S. Veprek, Proc. of the 4th Int. Symp. on Heating in Toroidal Plasmas, Roma ed. by ENEA Varenna Italy, Vol. I, 137 (1984).
25. C. Mercier, Nuc. Fusion **1**, 46 (1960).

Figure Captions

Fig. 1 Field aligned geometry used for the wave propagation equations.

Fig. 2 Dispersion branches $\omega^2(m,n;r) = R^{-2}v_A^2(r)[m + n/g(r)]^2$ in the continuum regime. The intersection points of these branches with the line $\omega^2 = \omega_0^2$ define a family of degenerate modes that also includes the narrow side bands around the intersection points plus potentially degenerate modes of higher m marked by crosses.

Fig. 3 A simple one-dimensional example of degeneracy and gap formation: the energy spectrum of an electron in a periodic potential.

Fig. 4 The spectrum of MHD continuum in a cylinder showing the two levels of degeneracy: (i) Degeneracy between equal ω^2 of opposite $k_{||}$. These frequencies can not be coupled by a poloidal variation and do not lead to gap formation (ii) Degeneracy among modes of different poloidal numbers m leading to strong coupling.

Fig. 5 The spectrum of the toroidal modes. Each branch Ω_i^2 contains three segments of different helicity and resonant surface. Positions $q_1^{(1)}$ $q_1^{(2)}$ $q_1^{(3)}$ show the resonant surfaces of the mode Ω_1; $q_1^{(2)}$ $q_2^{(2)}$, $q_3^{(2)}$ show the displacement of one of the resonant surfaces (m_2) relative to its generic position for each toroidal mode Ω_1, Ω_2, Ω_3.

Fig. 6 Case of intersecting branches (a) First level of diagonalization around the intersection point leads to gap formation (b) Second diagonalization of remaining degeneracy mixes all three modes modifying the width of the gap.

Fig. 7 Schematic illustration of the transition from cylindrical to toroidal eigenmodes using only three modes for simplicity. The wave component perpendicular to both the magnetic field and the radial direction, $E_\perp(r)$, is plotted versus the radius r. (a) Three degenerate cylindrical modes of the same frequency ω and toroidal wave number n with different poloidal wave numbers $m-1$, m, and $m+1$ respectively, each one localized around the associated resonant layer. (b) The modes resulting from the above cylindrical modes when toroidicity effects are included in

the wave propagation operator. Spectral perturbations of different poloidal number appear around each generic resonant surface. (c) The three toroidal modes formed by the three different linear superpositions of the modes in (b) due to the toroidal perturbation in the dielectric tensor. (d) Lowest order representation of the toroidal modes when only the zeroth order terms are kept in (c). This result can be obtained directly by the mixing of the purely cylindrical modes in (a). Note the departure of the new resonant surfaces from the generic position (vertical lines) in (c) and (d) if the frequency ω is kept fixed.

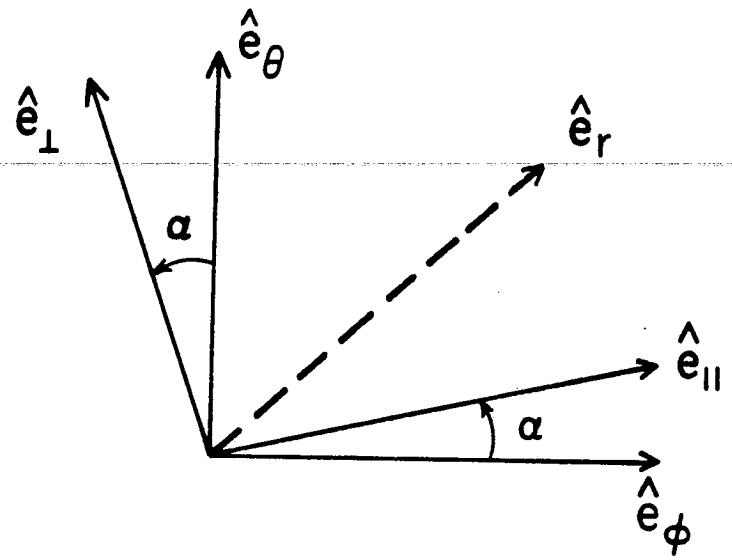
$\hat{e}_\theta$
$\hat{e}_\perp$
$\hat{e}_r$
α
$\hat{e}_{\parallel}$
α
$\hat{e}_\phi$

Fig. 1

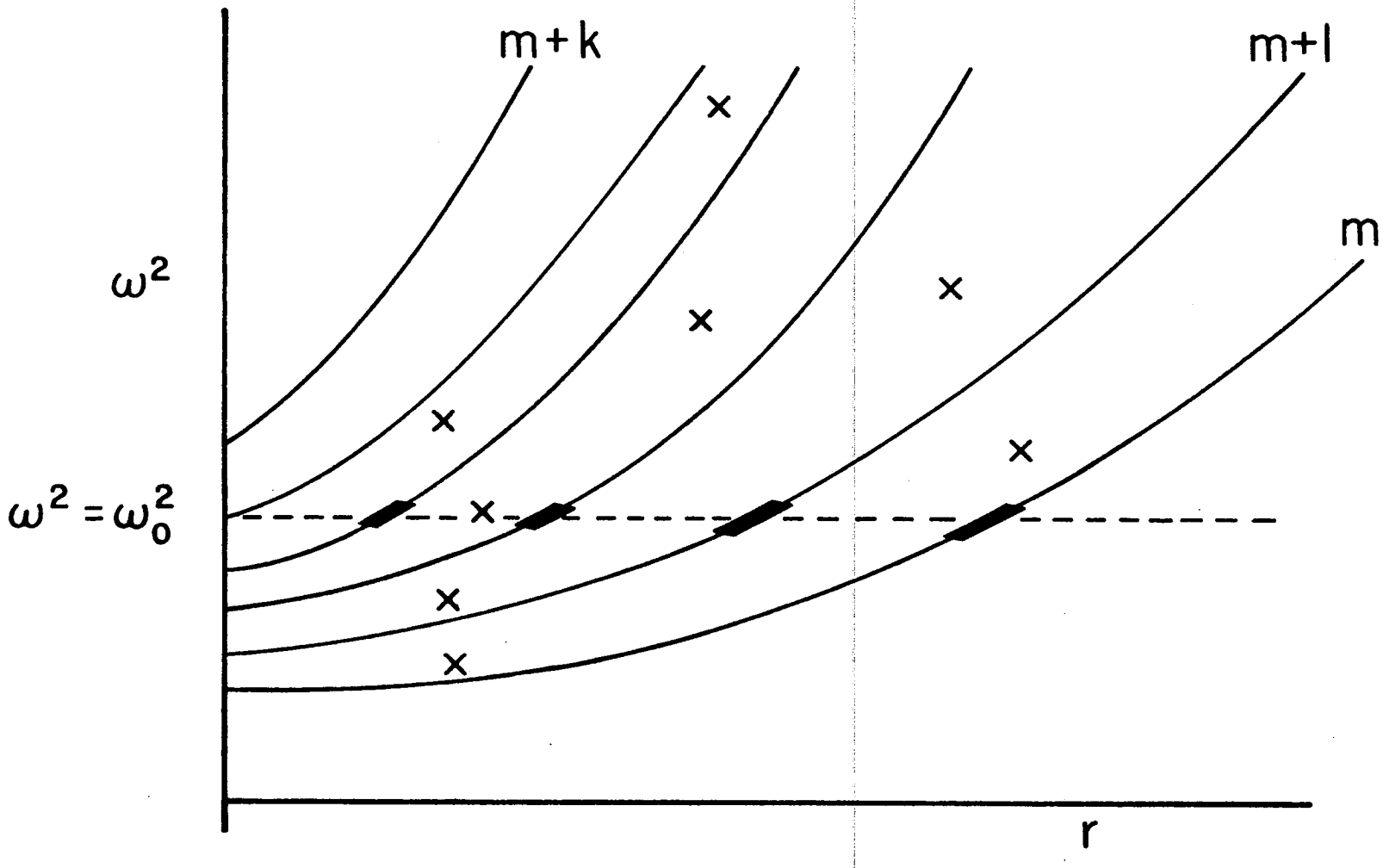

Fig. 2

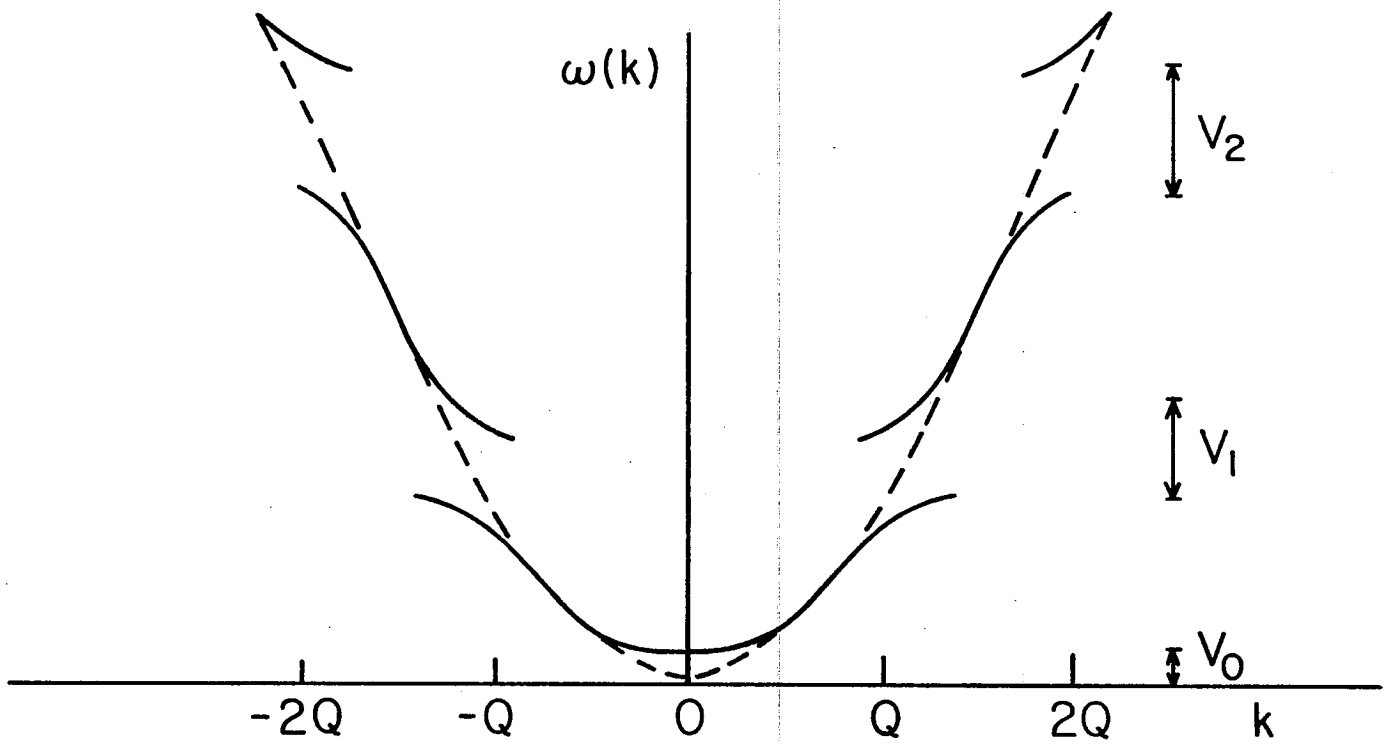

Fig. 3

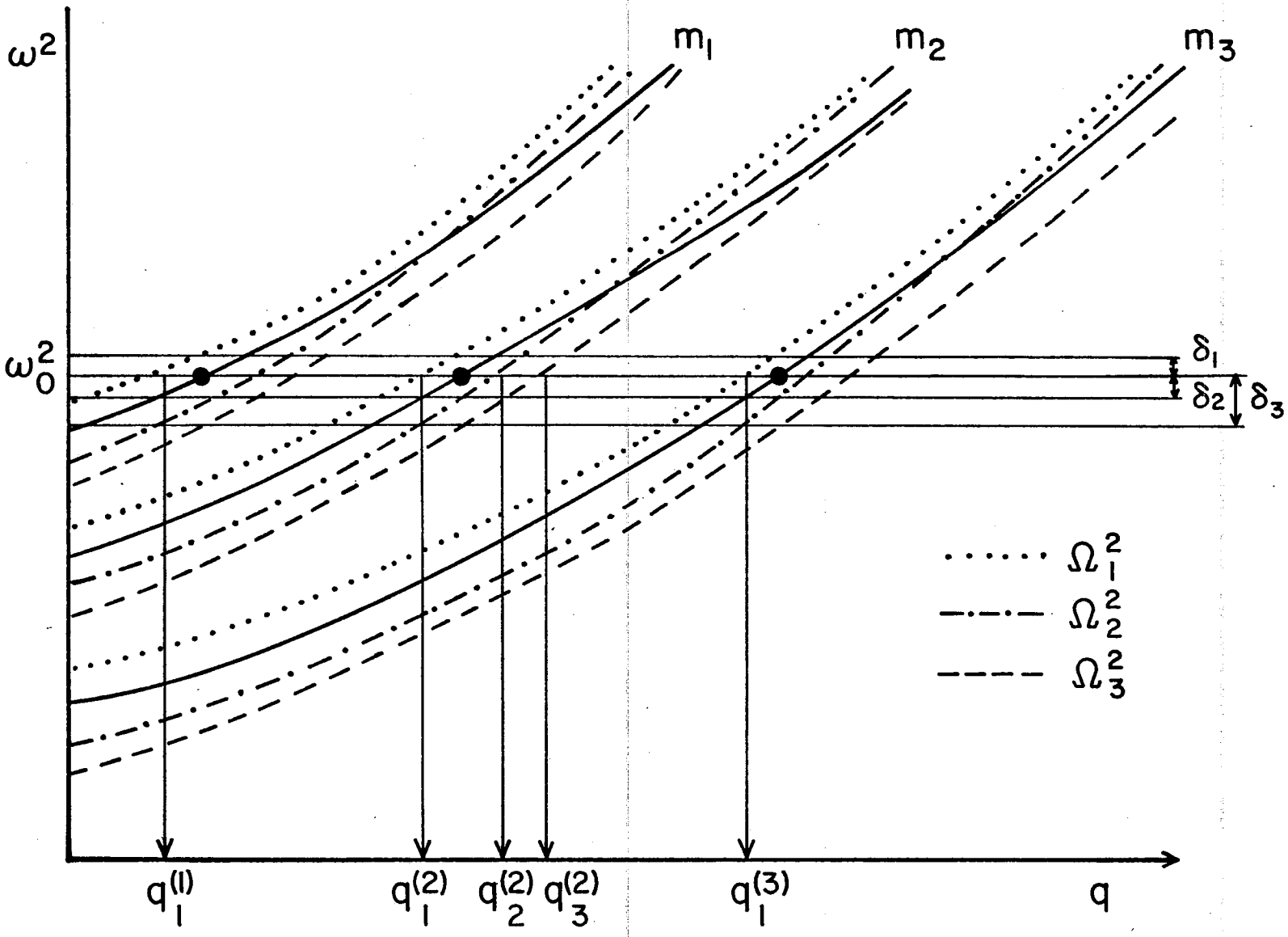
ω^2
m_1
m_2
m_3
ω_0^2
δ_1
δ_2
δ_3
Ω_1^2
Ω_2^2
Ω_3^2
$q_1^{(1)}$
$q_1^{(2)}$
$q_2^{(2)}$
$q_3^{(2)}$
$q_1^{(3)}$
q

Fig. 5

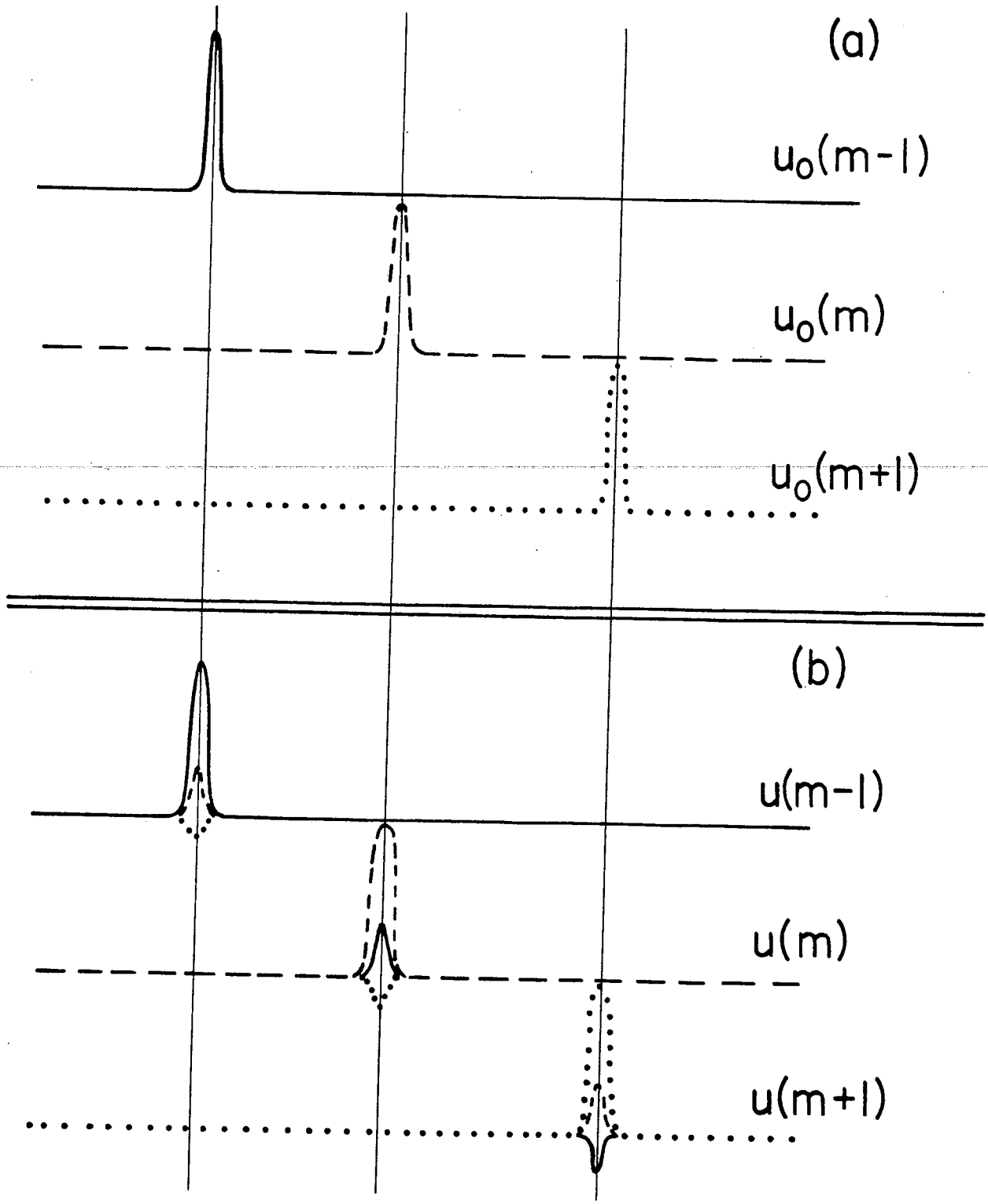

Fig. 7(a)-(b)

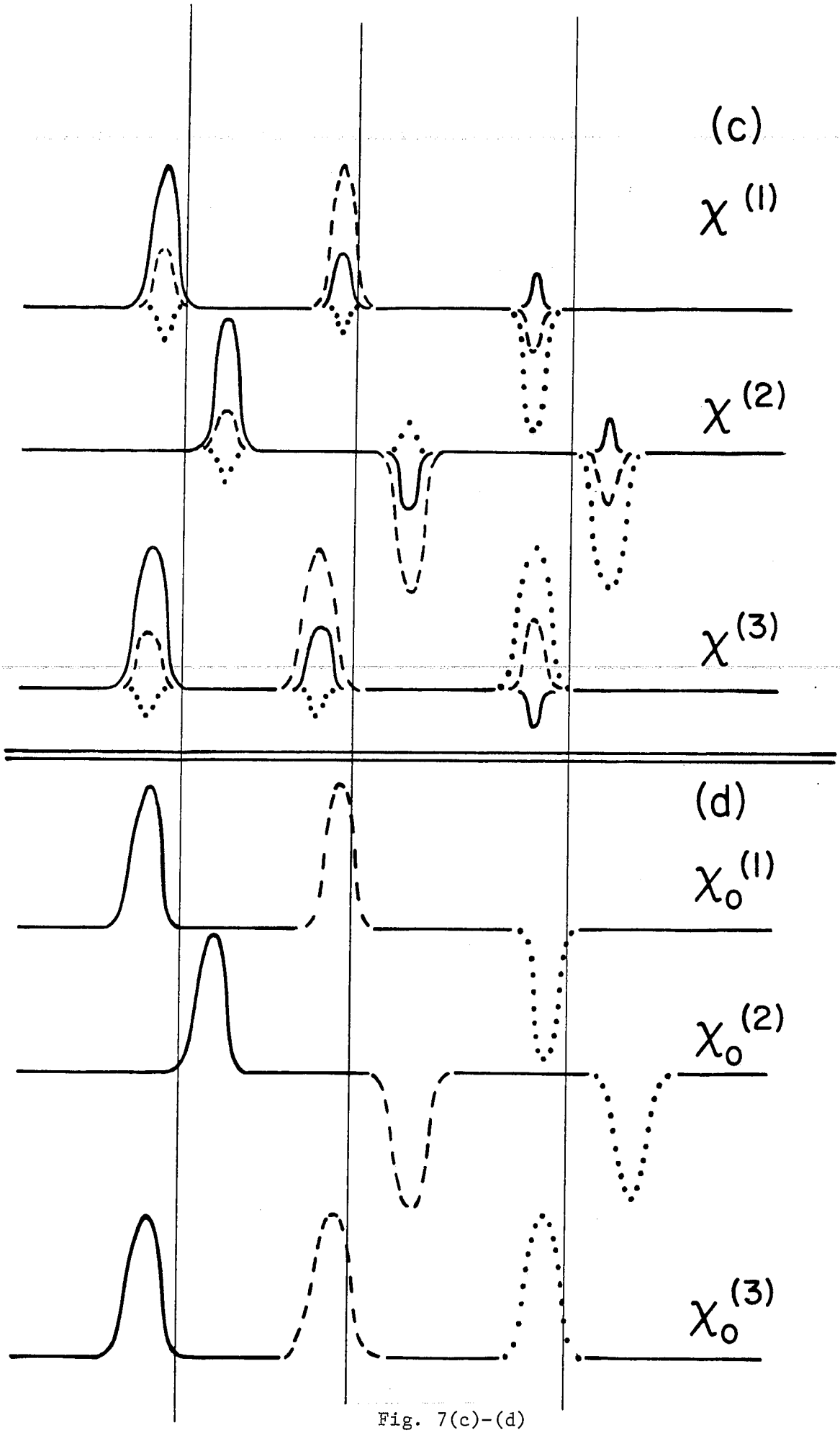

Fig. 7(c)-(d)